AMERICAN SOCIETY FOR MICROBIOLOGY | Journal of Virology

Veterinary Microbiology | Full-Length Text

Micropterus salmoides rhabdovirus enters cells via clathrin-mediated endocytosis pathway in a pH-, dynamin-, microtubule-, rab5-, and rab7-dependent manner

Jian-Fei Lu,[1,2,3] Sheng Luo,[1,2,3] Hao Tang,[1,2,3] Jia-Hui Liang,[1,2,3] Yi-Fan Zhao,[1,2,3] Yang Hu,[1,2,3] Guan-Jun Yang,[1,2,3] Jiong Chen[1,2,3]

AUTHOR AFFILIATIONS See affiliation list on p. 16.

ABSTRACT *Micropterus salmoides* rhabdovirus (MSRV) is an important fish pathogen that infects largemouth bass. To date, the entry process for MSRV remains obscure. Here, the dynamic process of MSRV entry and internalization was analyzed using biochemical inhibitors, RNA interference, and single-virus tracking technology. Accordingly, DiD was used as a fluorescent label for sensitive, long-term tracking of MSRV entry in living cells. The motion analysis suggested that MSRV initially experiences slow movement in the cell periphery, while it undergoes relatively faster and directed motion toward the cell interior, dependent on the microtubule. Besides, our data demonstrated that the MSRV enters epithelioma *papulosum cyprinid* (EPC) cells via clathrin-mediated endocytosis in a low pH-, dynamin-, and clathrin-dependent manner. Furthermore, after endocytosing into EPC cells, MSRV moves along the classical endosome/lysosome trajectory. This study reveals the entry pathway and intracellular dynamics of MSRV in EPC cells, providing new insights into the infection mechanism of rhabdoviruses.

IMPORTANCE Although *Micropterus salmoides* rhabdovirus (MSRV) causes serious fish epidemics worldwide, the detailed mechanism of MSRV entry into host cells remains unknown. Here, we comprehensively investigated the mechanism of MSRV entry into epithelioma *papulosum cyprinid* (EPC) cells. This study demonstrated that MSRV enters EPC cells via a low pH, dynamin-dependent, microtubule-dependent, and clathrin-mediated endocytosis. Subsequently, MSRV transports from early endosomes to late endosomes and further into lysosomes in a microtubule-dependent manner. The characterization of MSRV entry will further advance the understanding of rhabdovirus cellular entry pathways and provide novel targets for antiviral drug against MSRV infection.

KEYWORDS endocytosis, *Micropterus salmoides* rhabdovirus, single-virus tracking, clathrin-mediated endocytic, endosome trafficking

Viral infection is initiated by the specific adsorption of viral envelope protein to a receptor, followed by the transportation of virus into target cells and the subsequent uncoating of the virion to release viral genomes (1, 2). Endocytosis is a biological process mediating cellular internalization events, which can be utilized by viruses for their entry into host cells. Knowledge of the endocytosis pathway is necessary to enhance our understanding of the interaction between virus and host cell (3, 4).

Most rhabdovirus hijack host endocytic pathways to overcome the membrane barriers of target cell. There are several endocytic pathways, including clathrin-mediated endocytosis (CME), micropinocytosis, caveola-mediated endocytosis, and clathrin or caveola-independent endocytosis (5, 6). Some viruses can use multiple pathways to internalize, while others can even use different endocytic pathways when entering

Editor Rebecca Ellis Dutch, University of Kentucky College of Medicine, Lexington, Kentucky, USA

Address correspondence to Jiong Chen, jchen1975@163.com.

Jian-Fei Lu and Sheng Luo contributed equally to this article. Author order was determined alphabetically.

The authors declare no conflict of interest.

See the funding table on p. 17.

Received 14 May 2023
Accepted 23 July 2023
Published 21 September 2023

cells from different tissues (7, 8). Clathrin-mediated endocytosis is a classical endocytic pathway used by viruses as the primary means of internalization. In this pathway, viruses are internalized via clathrin-coated pits (CCP) after the viral particle binds to receptors on the plasma membrane. The intracellular clathrin-coated vesicle (CCV) is formed after the CCP invagination and is being pinched off from the cell membrane. After that, the CCV sheds its clathrin-coat subunits, followed by the process of acidification and transportation (9).

In classical clathrin-mediated endocytosis, the step from early to late endosomes is essential for the selective trafficking of cargo and membrane complex to lysosomes for degradation (10). The dynamics of endocytic trafficking are finely regulated by Rab proteins, which are small GTPases of the Ras superfamily (11). Numerous reports have shown that viruses hijack Rab proteins during the invasion, including viral entry by endocytosis, assembly, and egress (12). Ras-related protein 5 (Rab5) has been reported to be localized in the early endosomes, which is involved in the formation of CCV and regulated the transport of newly endocytosed vesicles from the plasma membrane to early endosomes (13, 14). Ras-related protein 7 (Rab7) is a late endosome-/lysosome-associated small GTPase involved in the transport to late endosomes and lysosomes (15, 16).

Rhabdoviruses, members of the order Mononegavirales, have been isolated from a wide variety of hosts, including mammals, birds, reptiles, teleosts, mollusks, insects, and plants (17). *Micropterus salmoides* rhabdovirus (MSRV), a highly pathogenic member of the genus *Perhabdovirus* in the family *Rhabdoviridae*, causes acute mass mortality in populations of largemouth bass (18, 19). The first report of MSRV epidemic occurred at a largemouth bass hatchery in China in 2014. Nowadays, the increasing expansion of diseases caused by MSRV infection has led to serious economic losses to the aquaculture industry (20, 21). There are many studies on the mechanism of host cell invasion by the family *Rhabdoviridae* (5, 22–24), but only a few of them focus on the genus *Perhabdovirus*. Persistent MSRV infection has been demonstrated in epithelioma *papulosum cyprinid* (EPC) cells, and numerous studies of MSRV have been conducted in EPC cells (20, 25). However, little is known about the early events of MSRV infections and their mechanisms for MSRV internalization into host cells.

Here, the single-virus tracking, molecular, and pharmacological methods have been combined to investigate the internalization mechanism of MSRV entry into EPC cells. Our results indicated that MSRV entry into EPC cells is dependent on clathrin-mediated endocytosis, low pH, microtubule, early/late endosomes, and lysosomes, but not caveola-mediated endocytosis or macropinocytosis. Together, the results improve our understanding of the mechanisms of MSRV internalization into EPC cells.

RESULTS

Characterization of labeled MSRV and real-time tracking of MSRV

In order to visualize the cell entry process of MSRV, we labeled MSRV with 1,1′-dioctadecyl-3,3,3′,3′-tetramethylindodicarbocyanine,4-chlorobenzenesulfonate salt (DiD). The results of transmission electron microscope (TEM) showed that the purified DiD-MSRV particles also kept intact structure compared with unlabeled MSRV (Fig. 1A), indicating that the labeling approach does not interfere with viral biological structure. Meanwhile, MSRV viral RNA of unlabeled MSRV and DiD-MSRV were determined by real-time quantitative PCR (RT-qPCR). There was no significant difference between unlabeled and labeled MSRV (Fig. 1B) at different time points, suggesting the viral infectivity of DiD-MSRV is not affected by the DiD conjunction.

Single-virus tracking in real-time allows us to explore the dynamic process of viruses in the cytoplasm (26, 27). Here, MSRV transport in EPC cells was tracked by real-time imaging at the single virus level. Snapshots showed that a single particle of DiD-MSRV attached to the cell membrane and was immediately internalized into the cell cytoplasm (Fig. 1C; Video S1). The initial motion of virus attachment was slow (blue curve, 0.018 μm/s). After entering the cell, the virus underwent a relatively rapid (red curve,

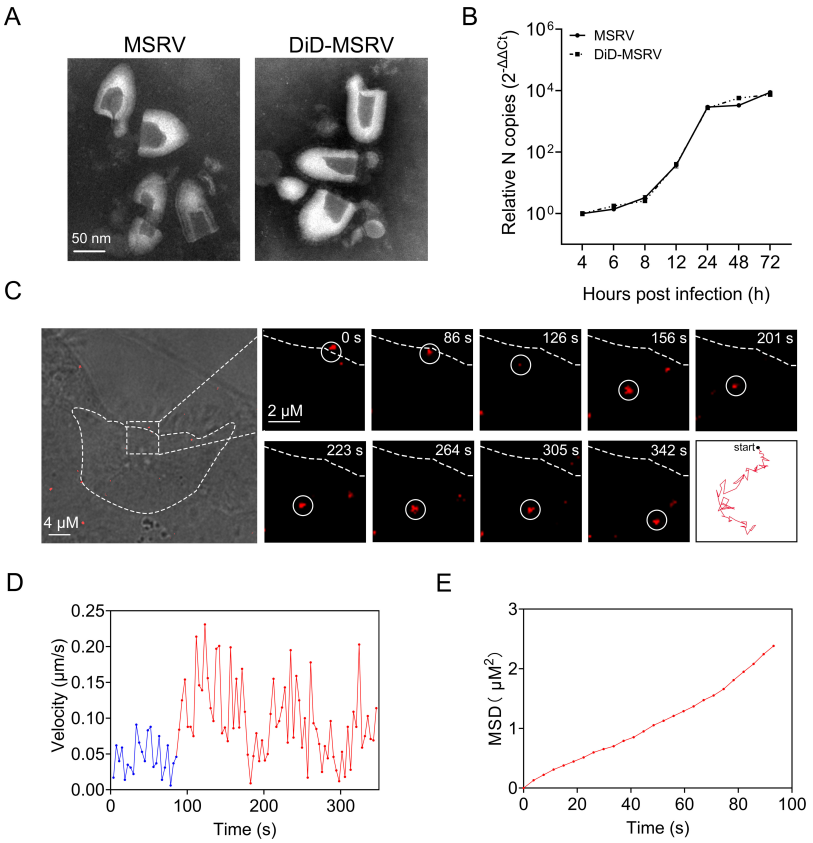

FIG 1 Characterization of labeled MSRV and real-time tracking of MSRV. (A) Transmission electron microscope images of unlabeled MSRV (left) and DiD (1,1′-dioctadecyl-3,3,3′,3′-tetramethylindodicarbocyanine,4-chlorobenzenesulfonate salt) labeled MSRV (right). Scale bars represent 50 nm. (B) Viral infection of DiD-MSRV in epithelioma *papulosum cyprinid* (EPC) cells. Cells were infected with MSRV at a multiplicity of infection (MOI) of 0.1. Viral RNA copy number was determined by RT-qPCR at 4, 6, 8, 12, 24, 48, and 72 hpi. (C) Confocal images of DiD-MSRV in MSRV infected EPC cells. White circles indicate the position of the virus. Dashed lines represent the plasma membrane. Red lines indicate the typical trajectories of virus. Scale bar = 2 μm. (D) Instantaneous velocity of the virus. Blue and red lines separately represent the slow and rapid movement of virus. (E) Mean-squared displacement (MSD)-time plots of viral movement.

0.048 μm/s) and directed movement in the cytoplasm (Fig. 1D and E). The results demonstrated that DiD-MSRV underwent directed movement toward the cell interior, and the movement was a slow-fast process. The results indicated that DiD-MSRV could be used for real-time tracking virus in live EPC cells.

MSRV entry into EPC cells is low pH-dependent

To initiate efficient infection, many viruses utilize the acidic environment of the endosomal system to enter cells (22, 27, 28). In order to assess whether MSRV entry is pH-dependent, EPC cells were first pretreated with the weakly basic amines NH_4Cl or the acidification of endosomal vesicles inhibitor chloroquine (CQ), then cells were infected with MSRV. The results showed that NH_4Cl did not impact cell viability at concentrations of 20 mM or lower, whereas the working concentrations of CQ ranged from 0 to 20 μM (Fig. 2A). Both inhibitors reduced MSRV infection in a dose-dependent manner compared with the level in control cells. A concentration of 20 mM NH_4Cl or 20 μM CQ led to 99.99% or 98.78% reduction of the viral RNA, respectively (Fig. 2A). Similarly, both inhibitors reduced viral protein synthesis in a dose-dependent manner (Fig. 1B and C).

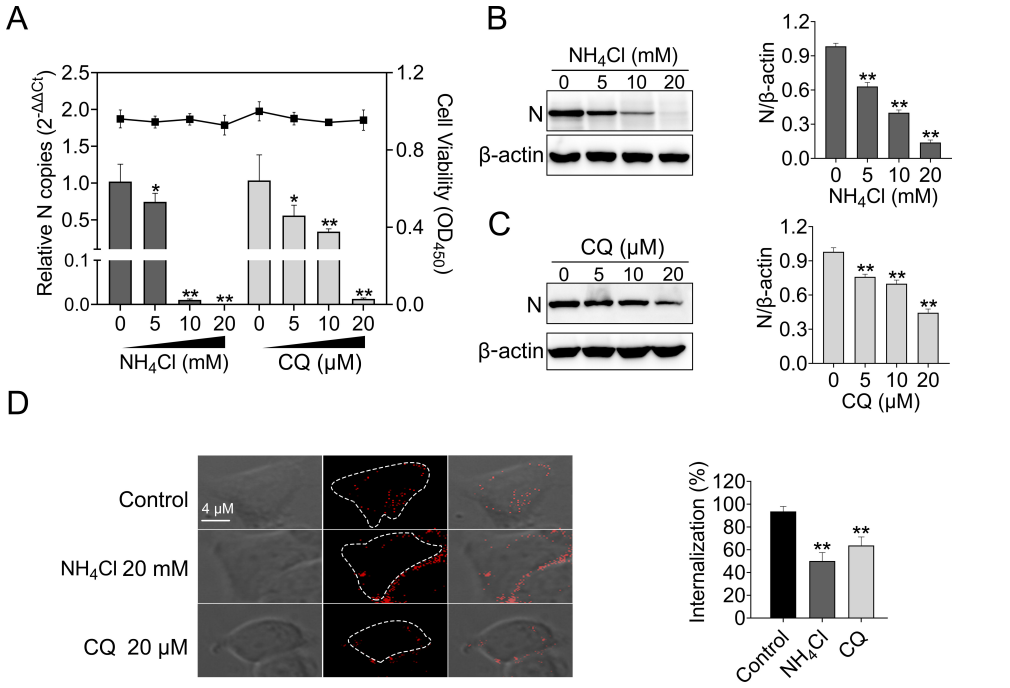

FIG 2 MSRV entry into EPC cells depends on low-pH. (A, B, and C) NH_4Cl and chloroquine (CQ) inhibited MSRV infection. Cells were pretreated with indicated concentrations of NH_4Cl and CQ at 25°C for 2 h and then infected with MSRV (MOI of 0.1) at 25°C for 2 h. At 24 hpi, cells were lysed to detect viral RNA by RT-qPCR and N protein by western blotting (WB). The cell viability of the indicated inhibitors was determined individually using cell counting Kit 8 (CCK-8). The expression of MSRV N protein was quantified by normalizing to β-actin and relative to the control-treated group. (D) NH_4Cl and CQ attenuated the internalization of MSRV. Cells were pretreated with NH_4Cl (20 mM) or CQ (20 μM) for 2 h, then incubated with DiD-MSRV (MOI of 50) for 0.5 h in the presence of inhibitor, and the fluorescence was determined by confocal fluorescence microscopy. Images were analyzed with ImageJ, and internalization of MSRV was calculated by measuring the percentage of intracellular fluorescence intensity to whole-cell fluorescence intensity. Thirty cells were depicted in each experiment and three independent experiments were carried out. Error bars represent standard deviations. *, $P < 0.05$; **, $P < 0.01$.

Furthermore, we investigated the effect of pH on the internalization of MSRV. In EPC cells infected with DiD-MSRV (pretreated with NH_4Cl or CQ) a pattern of fluorescence signal remained on the cell membrane but failed to reach the cytoplasm (Fig. 2D). Further statistical analyses were performed to calculate the internalization rate of DiD-MSRV. In the presence of endosome acidification inhibitors, the internalization rate was apparently reduced, with a rate of 50.11% for NH_4Cl and 63.76% for CQ, respectively (Fig. 2D). This result indicated that internalization of the DiD-MSRV is effectively suppressed by NH_4Cl or CQ.

MSRV entry depends on dynamin

Dynamin is a GTPase that is responsible for endocytosis, especially in cellular membrane fission during vesicle formation. Dynamin has been demonstrated to be required in the internalization of numerous viruses (29). Thus, we explored the role of dynamin in MSRV entry. Dynasore, a cell-permeable non-competitive dynamin GTPase activity inhibitor (30), was used in this study. EPC cells were treated with increasing concentrations of dynasore, and the cytotoxicity test showed that dynasore did not impact cell viability at concentrations of 100 μM or lower (Fig. 3A). Next, EPC cells were treated with dynasore and infected with MSRV, followed by detecting viral RNA with RT-qPCR and protein with western blotting (WB). As shown in Fig. 3A and B, a dose-dependent reduction of viral RNA and protein levels was observed in dynasore-treated groups.

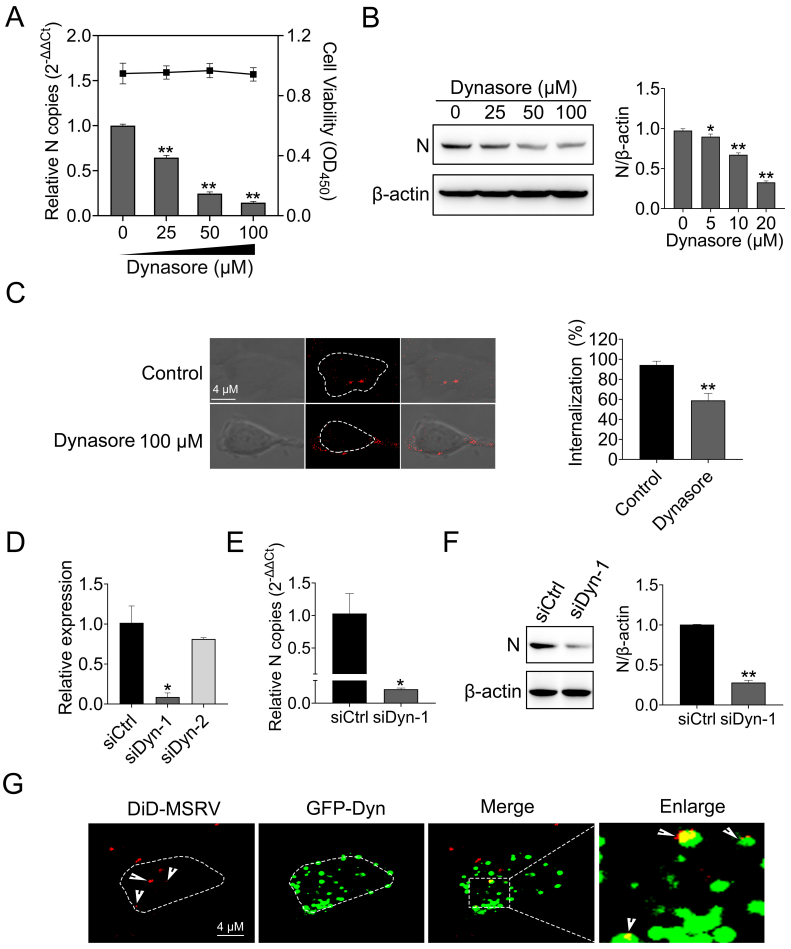

FIG 3 MSRV entry depends on dynamin. (A and B) Dynasore inhibited MSRV infection. Cells were pretreated with indicated concentrations of dynasore for 2 h and then infected with MSRV (MOI of 0.1) for 2 h at 25°C. At 24 hpi, cells were lysed to detect viral RNA copy by RT-qPCR and N protein by WB. The cell viability of the dynasore was determined using CCK-8. (C) Dynasore attenuated the internalization of MSRV. Cells were pretreated with dynasore (100 μM) for 2 h, then incubated with DiD-MSRV (MOI of 50) for 0.5 h, and the fluorescence was determined by confocal fluorescence microscopy. (D, E, and F) Dynamin knockdown restrained MSRV infection. siDyn or siCtrl-transfected cells were infected with MSRV (MOI of 0.1) for 24 h. Cells were lysed to determine viral RNA by RT-qPCR and N protein by WB. The presented results represent the means and standard deviations of data from three independent experiments. *, $P < 0.05$; **, $P < 0.01$. (G) The colocalization of MSRV with dynamin. Cells were transfected with pEGFP-Dyn and incubated with DiD-MSRV for 30 min at 25°C before imaging.

In the internalization assay, the fluorescence signal of DiD-MSRV transferred to the cytoplasm in control cells, while the fluorescence signal of DiD-MSRV distributed at the cell periphery in dynasore-treated cells. The internalization rate in dynasore-treated cells was 37.46% in comparison with the control group (Fig. 3C). Moreover, we evaluated the role of dynamin in MSRV infection. RT-qPCR demonstrated the validity of siRNA-mediated knockdown of dynamin (Fig. 3D). Compared with siCtrl, siDyn-1 significantly decreased MSRV infection, as evidenced by the notably reduced viral RNA and protein expression (Fig. 3E and F). The localization of MSRV with dynamin was analyzed by confocal microscopy. As shown in Fig. 3G, the colocalization of DiD-MSRV and GFP-Dyn was observed. These results indicated that MSRV entry into EPC cells is dynamin-dependent.

MSRV enters EPC cells via clathrin-mediated endocytosis

We further investigated whether MSRV enters EPC cells via clathrin-mediated endocytosis. This is because dynamin has been reported to participate in both clathrin- and caveolin-mediated endocytosis, and some rhabdovirus have been established to infect through clathrin-mediated endocytosis (31, 32). First of all, cell viability upon chlorpromazine (CPZ) or sucrose (specificity inhibitor of clathrin-mediated endocytosis) treatment was determined to exclude cytotoxic effects. EPC cell viability remained unchanged at up to 10 μM for CPZ and 200 mM for sucrose (Fig. 4A), as expected. Cells were treated with CPZ or sucrose and infected with MSRV, followed by detecting viral RNA with RT-qPCR and protein with WB. Both CPZ and sucrose suppressed MSRV infection in a dose-dependent manner. A concentration of 10 μM CPZ or 100 mM sucrose led to 99.4% or 97.2% reduction of viral RNA copies (Fig. 4A). Similarly, both inhibitors reduced viral protein synthesis in a dose-dependent manner (Fig. 4B and C). Next, the effect of clathrin-mediated endocytosis on the internalization of MSRV was analyzed by confocal microscopy. The cells were pretreated with 10 μM CPZ or 100 mM sucrose, then infected with DiD-MSRV, and finally the fluorescence was determined by confocal microscopy. In CPZ- or sucrose-treated cells, the fluorescence signal rested on the cell periphery, while the fluorescence signal transferred to the cytoplasm in control cells. After inhibitor treatment, the internalization rate of MSRV was reduced by 61% for CPZ and 31% for sucrose, respectively (Fig. 4D).

Clathrin is a protein that plays a critical role in the formation of CCP and CCV. Clathrin heavy chain (CHC) and light chain (CLC) form a triskelion shape, which is a vital component for regulating the formation and disassembly of the clathrin lattice (33). Here, we assessed the role of clathrin during MSRV infection by siRNA knockdown of CLC. Depletion of CLC in EPC cells was confirmed by RT-qPCR (Fig. 4E). Besides, EPC cells were transfected with siCLC or siCtrl and then infected with MSRV at a multiplicity of infection (MOI) of 0.1. MSRV RNA levels were quantitated by RT-qPCR and protein was detected by WB. Figure 4F and G show that viral RNA and protein decreased significantly in siCLC-transfected cells compared to those in siCtrl-transfected cells. Finally, confocal microscopy was used to detect the colocalization of MSRV with CLC. DiD-MSRV (red) colocalized with GFP-CLC (green) was observed in Fig. 4H. Taken together, these results showed MSRV entry into EPC cells through clathrin-mediated endocytosis.

MSRV entry into EPC cells is caveola-mediated endocytosis independent

Except for clathrin-mediated endocytosis, dynamin was also implicated in caveola-mediated endocytosis (34), so the role of caveola-mediated endocytosis during MSRV entry into EPC was evaluated in the following experiment. EPC cells were treated with various concentrations of genistin and nystatin [with known functions of disrupting the caveola-mediated endocytosis (35)] for 2 h, followed by MSRV infection. At 24 h post infection (hpi), viral RNA was determined via RT-qPCR and proteins were detected by WB. The results of the cellular viability assay showed that EPC cells tolerated up to 100 μM genistin and 20 μM nystatin (Fig. 5A). Moreover, there was no significant reduction in the number of MSRV RNA in EPC cells when genistin or nystatin was present, indicating that genistin or nystatin negatively inhibit MSRV infection. Meanwhile, a similar phenomenon appeared in the expression of protein (Fig. 5B and C). In addition, the effect of caveola-mediated endocytosis on the internalization of MSRV was analyzed. As demonstrated by confocal fluorescence microscopy, all the DiD-MSRV fluorescence signal was internalized to cytoplasm in a different group (Fig. 5D), indicating genistin and nystatin have no effect on MSRV internalized to EPC cells.

Caveolae are composed of caveolin membrane proteins that can bud from the plasma membrane to form vesicles and participate in the entry of viruses. Caveolin-1 is important for the formation and stability of caveolae (36). The localization of MSRV with caveolin-1 was analyzed by confocal microscopy. As shown in Fig. 5E, there was no colocalization between DiD-MSRV and GFP-Cav in EPC cells. These results turned out that the entry of MSRV into EPC cells is independent of caveola-mediated endocytosis.

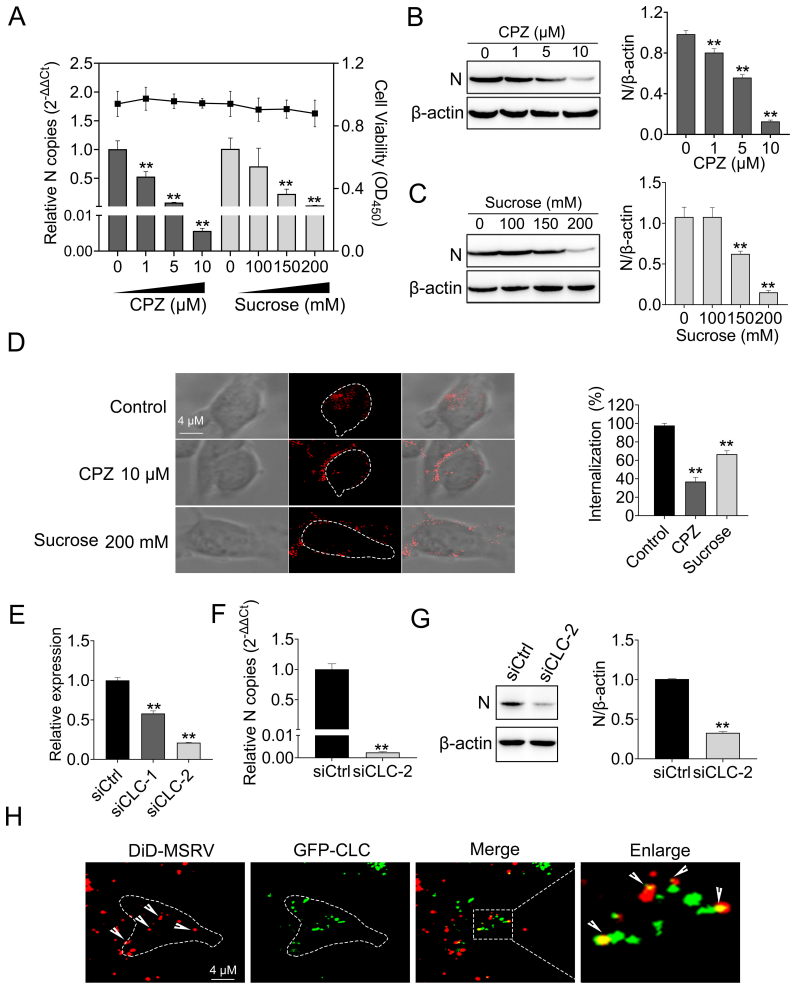

FIG 4 MSRV enters EPC cells via clathrin-mediated endocytosis. (A, B, and C) Chlorpromazine (CPZ) and sucrose inhibited MSRV infection. EPC cells treated with increasing concentrations of CPZ or sucrose were incubated with MSRV for 2 h at 25°C. At 24 hpi, cells were lysed to detect viral RNA by RT-qPCR and N protein expression by WB. The cell viability of inhibitors was determined using CCK-8. (D) CPZ and sucrose suppressed the internalization of DiD-MSRV. Cells were incubated with DiD-MSRV for 0.5 h after pretreating with 10 μM CPZ or 100 mM sucrose for 2 h, the fluorescence was determined by confocal fluorescence microscopy. (E, F, and G) Clathrin light chain (CLC) knockdown inhibited MSRV infection. siCLC- or siCtrl-transfected cells were infected with MSRV. At 24 hpi, the cells were lysed to detect the viral RNA or N protein via RT-qPCR or WB, respectively. (H) The colocalization of MSRV with CLC. Cells were transfected with pEGFP-CLC and incubated with DiD-MSRV for 30 min at 25°C before imaging.

MSRV entry into EPC cells is macropinocytosis independent

Micropinocytosis is a non-selective endocytic pathway that mainly mediates fluid and membrane uptake under physiological conditions (37). Previous studies have shown that micropinocytosis is involved in rhabdovirus endocytosis (5). Here, 5-(N-methyl-N-isobutyl) amiloride (MIBA) and blebbistatin [with known functions of disrupting the micropinocytosis endocytosis (38)] were used to analyze the role of micropinocytosis during MSRV entry EPC cells. The cell viability of treated cells was unaffected by MIBA and blebbistatin at the concentrations used in these experiments (Fig. 6A). The effects of MIBA and blebbistatin on the replication of MSRV in EPC cells were tested as described above. The results of infection assay suggested that MIBA and blebbistatin had no impact on MSRV infection (Fig. 6A). Also, there was no significant difference between N protein expression among cells treated with inhibitors and control cells (Fig. 6B and C).

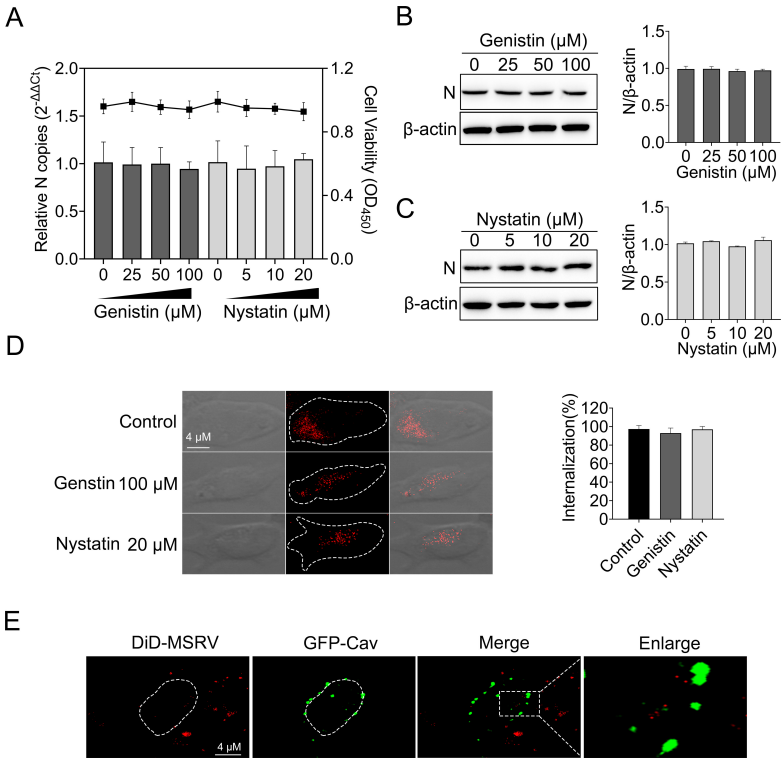

FIG 5 Caveola is not required for MSRV entry. (A, B, and C) Genistin and nystatin had no effect on MSRV infection. EPC cells were treated with indicated concentration of inhibitors for 2 h at 25°C. The cells were then incubated with MSRV (MOI = 0.1) in the presence of inhibitors for 2 h. Dimethyl sulfoxide (DMSO) was severed as the negative control. At 24 hpi, viral RNA was quantified by RT-qPCR and N protein was determined by WB. (D) Cells were incubated with 100 μM genistin or 20 μM nystatin and then infected with DiD-MSRV at MOI of 50. The internalization assay was performed as described above. The fluorescence signal of DiD-MSRV was determined by confocal fluorescence microscopy. (E) The colocalization of MSRV with caveolin-1. Cells were transfected with pEGFP-Cav and incubated with DiD-MSRV for 30 min at 25°C before imaging.

Furthermore, the results of internalization assay demonstrated no significant difference in the mean fluorescence intensity of DiD-MSRV between inhibitors and control cells (Fig. 6D). Together, MIBA and blebbistatin had no effects on infection and internalization of MSRV entry EPC cells, indicating that the endocytosis of MSRV in EPC cells is independent on macropinocytosis.

MSRV entry into EPC cells is microtubule-dependent

Upon internalization, many viruses are delivered to endosomal compartments and transported along the microtubule (22). Nocodazole disrupts microtubule by interfering with the polymerization of microtubule, thus restraining vesicular trafficking (39). To examine the potential role of microtubule in MSRV infection, we treated EPC cells with increasing concentrations of nocodazole prior to infection. As a result, the cell viability of treated cells was unaffected by nocodazole at the concentrations used in these experiments (Fig. 7A). Following the pretreatment with 10 μM nocodazole, viral RNA reduced to 99.8% of untreated cells. As expected, N protein expression was decreased by nocodazole in a dose-dependent manner (Fig. 7B).

To further investigate the role of the microtubule in MSRV entry into EPC cells, a tubulin-tracker was used to lab the microtubule. As shown in Fig. 7C through E; Video S2, DiD-MSRV particle retrograde transported along microtubule from the cell periphery to cell interior, implying MSRV was transported via a microtubule-dependent route. The trajectory analysis showed that the DiD-MSRV moved in a rapid and directional

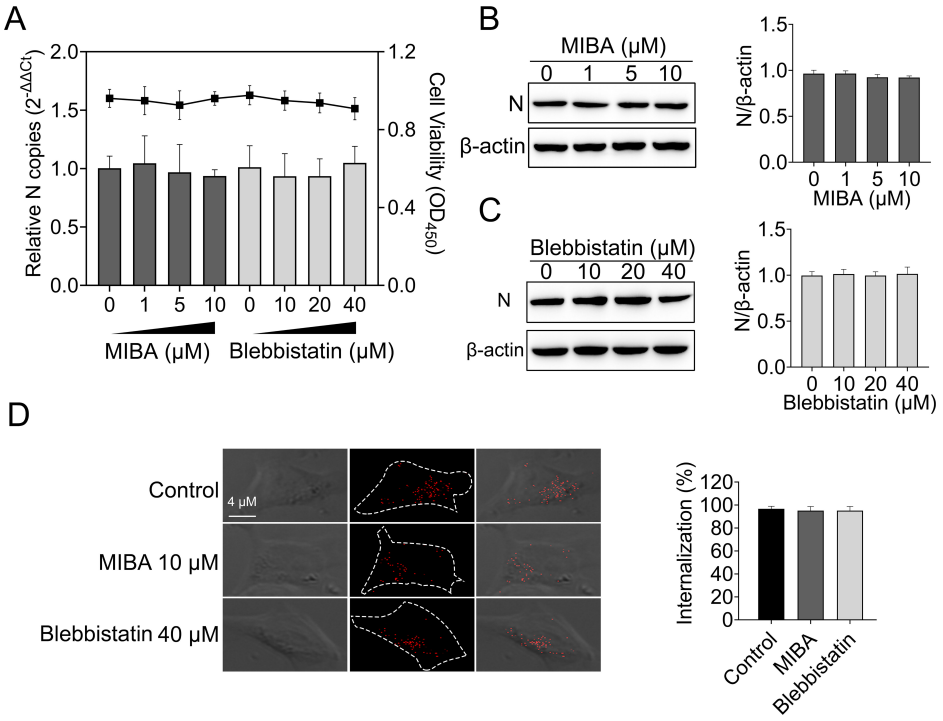

FIG 6 Macropinocytosis is not required for MSRV entry. (A, B, and C) 5-(N-methyl-N-isobutyl) amiloride (MIBA) and blebbistatin did not restrain MSRV infection. EPC cells were treated with indicated concentration of inhibitors for 2 h at 25°C. The cells were then incubated with MSRV (MOI = 0.1) in the presence of inhibitors for 2 h. DMSO was severed as the negative control. At 24 hpi, viral RNA was quantified by RT-qPCR and N protein was determined by WB. (D) Cells were incubated with 10 μM MIBA or 40 μM blebbistatin and then infected with DiD-MSRV at MOI of 50. The internalization assay was performed as described above. The fluorescence signal of DiD-MSRV was determined by confocal fluorescence microscopy.

movement along microtubule (red curve, 0.040 μm/s), and then moved slowly once the MSRV virions arrived at the intersections (blue curve, 0.018 μm/s). These results demonstrated that MSRV virions retrograde transport along microtubule from the cell periphery to cell interior.

Intracellular trafficking and the role of Rab5 and Rab7 in MSRV internalization

After identification of the internalization pathway hijacked by MSRV, we next tracked the transport vesicles utilized by incoming MSRV. Early endosomes mature into late endosomes by increasing the acidity of the cavity through proton pump activity. At the same time, late endosomes can become larger vesicles by fusing with the same type of endosomes and preparing to fuse with lysosomes (10, 40). Rab5 and Rab7 GTPases are required for the transport of endocytosed cargo to early or late endosomes (11, 41). Accordingly, we interfered with the expression of Rab5 involved in early endosomes and Rab7 involved in late endosomes. siRab5 obviously inhibited the expression of Rab5 in EPC cells (Fig. 8A), the suppression rates of siRab5-1 and siRab5-2 were 55% and 42%, respectively. Therefore, siRab5-2 was selected for the subsequent experiment (Fig. 8A). Similarly, siRab7-2 was selected (Fig. 8D). Quantification of MSRV RNA showed that knockdown of Rab5 or Rab7 significantly blocked virus infection (Fig. 8B and E), comparing to those in siCtrl-transfected cells. Also, the knockdown of Rab5 and Rab7 was accompanied by lower expression of MSRV N protein (0.66-fold and 0.68-fold, respectively). The above results demonstrated that the MSRV infection is inefficient when the transport pathway is suppressed by the knockdown of Rab5 or Rab7.

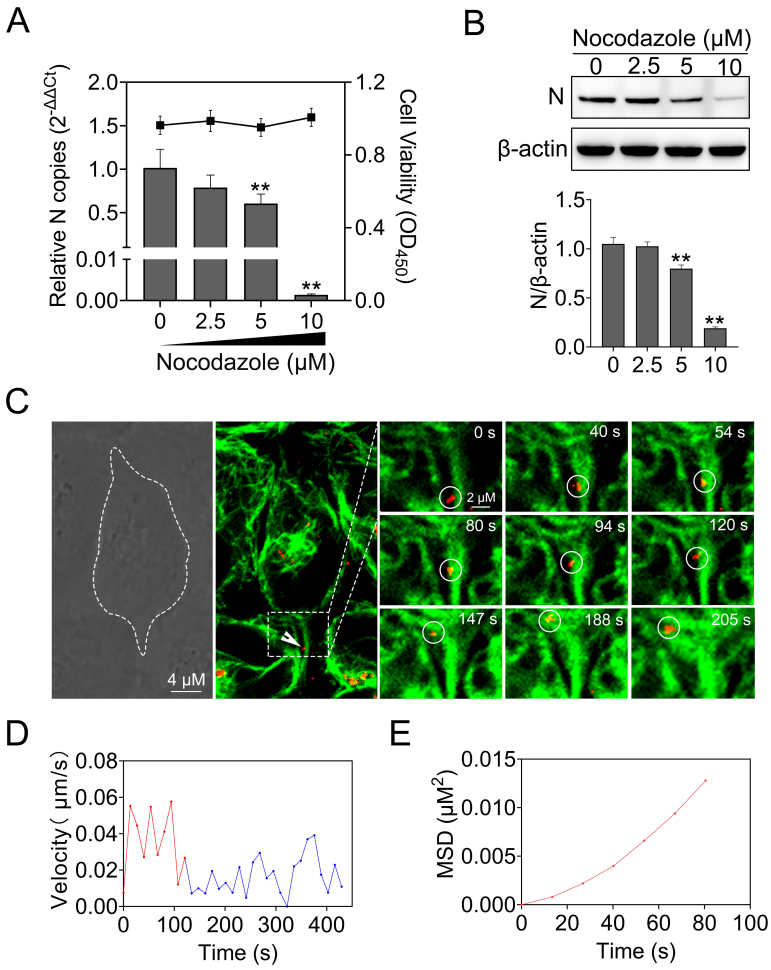

FIG 7 MSRV entry into EPC cells is microtubule dependent. (A and B) Nocodazole inhibited MSRV infection. Cells were pretreated with nocodazole at the indicated concentrations and then infected with MSRV in the presence of nocodazole. At 24 hpi, viral RNA was quantified by RT-qPCR and the level of N protein was analyzed by WB. The cell viability was determined using CCK-8. (C) Real-time imaging of DiD-MSRV transport along microtubule. Cells were incubated with tubulin-tracker for 1 h, and the unbound tracker was washed with phosphate-buffered saline. The cells were then incubated with DiD-MSRV (MOI = 50) at 25°C before imaging. The fluorescence was determined by confocal fluorescence microscopy. White circles indicate the position of the virus. Dashed lines represent the plasma membrane. (D) Instantaneous velocity of the virus. (E) MSD-time plots of viral movement.

We also identified whether viral particles co-located with early endosomes, late endosomes, and lysosomes. Here, the early endosomes and late endosomes were labeled by transfection with pEGFP-Rab5 and pEGFP-Rab7, respectively, lysosomes were stained with lyso-tracker. As shown in Fig. 9, the colocalization of DiD-MSRV with vesicle markers was observed from 5 to 30 min post infection. At 5 min post infection, MSRV particles colocalized with Rab5. At 15 min post infection, MSRV strongly colocalized with Rab5 or Rab7. At 30 min post infection, MSRV strongly colocalized with late Rab7 or lyso-tracker. DiD could insert into the phospholipid of the virus envelope to label the virus (8). After the fusion of the viral envelope with the endosome membrane and the subsequent release (uncoating) of the viral nucleocapsid, we were not sure whether the red fluorescence observed in the late endosomes and lysosomes was the viral envelope or the whole virion. To solve this problem, we studied the colocalization of MSRV N protein with early/late endosomes and lysosomes. The results showed that endogenous N protein colocalized with Rab5, Rab7, or lyso-tracker at 15 min post infection (Fig. S1). Altogether,

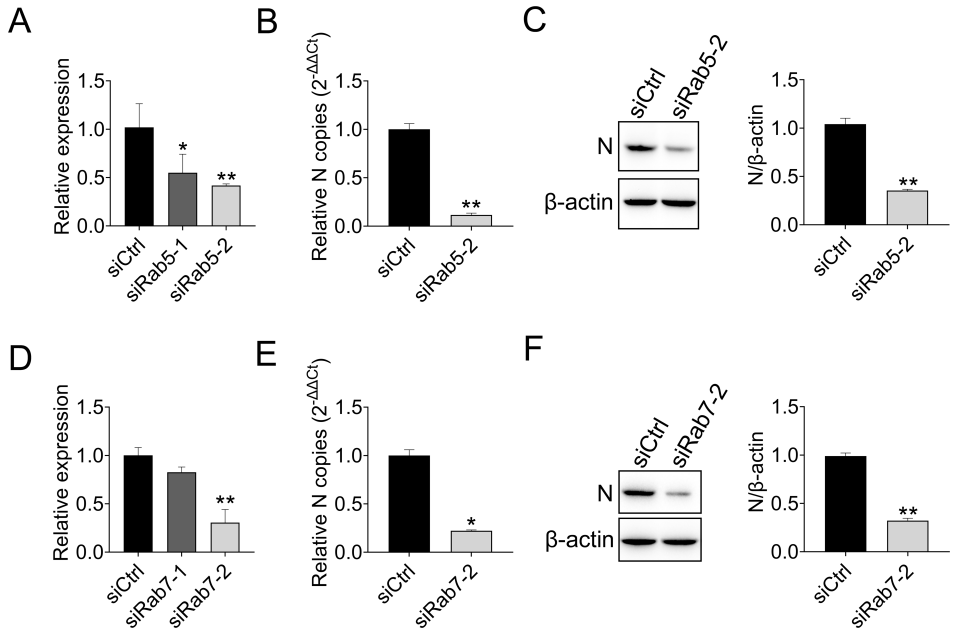

FIG 8 Rab5 and Rab7 are required for MSRV endocytosis. (A) The knockdown efficiency of Rab5. EPC cells were transfected with siCtrl, siRab5-1, or siRab5-2. At 24 h post transfection, the cells were collected for detecting the quantity of Rab5 by RT-qPCR. β-actin was used as the internal control. (B and C) Rab5 knockdown reduced the replication of MSRV. EPC cells were transfected with siRab5-2 or siCtrl, and infected with MSRV (MOI of 0.1) at 24 h post transfection. At 24 hpi, the viral RNA of infected cells was determined by RT-qPCR, and the N protein expression was detected by WB. (D) The knockdown efficiency of Rab7. The experiment procedure was the same as above. (E and F) Rab7 knockdown reduced the replication of MSRV. The experiment procedure was the same as above.

these data supported the idea that MSRV transports from early endosomes to late endosomes and further into lysosomes to initiate an infectious cycle.

DISCUSSION

Virus entry into host cell is the first step of infection and requires the synergistic action of several host cell factors. Thus, characterization of viral entry pathway is crucial for understanding virus pathogenesis and the development of antiviral drugs (39, 42). MSRV is a dominant pathogen causing a highly contagious largemouth bass disease and leading to considerable economic losses. However, little information is available about the pathway of MSRV entry into host cell. In this study, single-virus tracking in living cells was used to dynamically reveal the early stages of MSRV infection, including the endocytic pathway and endosome trafficking, which were previously not fully understood.

Enveloped virus entry into host cells through two different ways: endocytosis or membrane fusion mediated by enveloped glycoproteins (3). Previously, it was demonstrated that rabies virus (RABV) (28, 43), infectious hematopoietic necrosis virus (IHNV) (22), vesicular stomatitis virus (VSV) (44), bovine ephemeral fever virus (BEFV) (45), and Australian bat lyssavirus (ABLV) (46) enter cells via clathrin-mediated endocytosis, while spring viraemia of carp virus (SVCV) enters cells via clathrin-mediated endocytosis and micropinocytosis (5). Based on its similarity to other rhabdoviruses, we hypothesized that MSRV enters EPC cells by endocytosis. Endocytosis of most enveloped viruses requires an acidic endosomal environment to trigger fusion of the viral envelope with the endosome membrane, followed by internalization into the cytoplasm (3). As demonstrated in the previous study, the infection of BEFV is restrained by NH_4Cl, suggesting that BEFV entry is mediated by low pH and needs pH-triggered fusion (45). In this study, treatment of chemical inhibitors (CQ and NH_4Cl) reduced MSRV internalization and propagation,

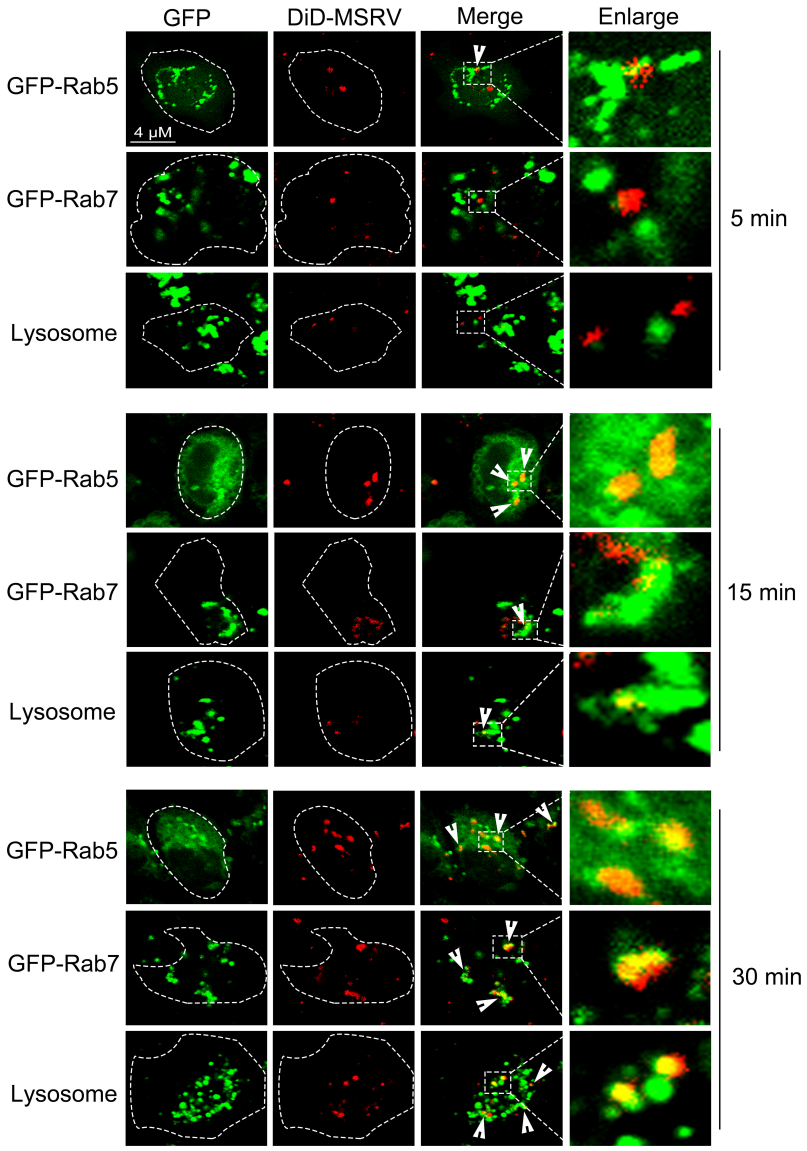

FIG 9 Co-localization of DiD-MSRV and endosome-lysosome. For Rab5 and Rab7, EPC cells were transfected with pEGFP-Rab5 or pEGFP-Rab7, and infected with DiD-MSRV 24 h post transfection. For lysosome, EPC cells were treated with lyso-tracker for 30 min, followed by DiD-MSRV infection. The fluorescence signal was observed by LSM880. Red signal: DiD-MSRV; green signal: Rab5, Rab7, or lysosome.

indicating that low pH in endosomes is required for MSRV infection. To further investigate whether MSRV utilized clathrin-mediated endocytosis to enter cells, we used chemistry inhibitors (CPZ or sucrose) or knockdown CLC by siRNA to specifically interfere clathrin-mediated endocytosis in EPC cells. We found that there was a downward trend in MSRV internalization and propagation when clathrin-mediated endocytosis was interfered. Therefore, we propose that MSRV enters EPC cells through clathrin-mediated endocytosis in a pH-dependent manner.

Dynamin is a high-molecular-weight GTPase that mediates the pinch of endocytic vesicles from plasma membranes during clathrin-mediated endocytosis and lipid raft/caveola-based endocytosis (47). However, little is currently known about the involvement of dynamin in the MSRV entry. Here, using chemistry inhibitor (dynasore) and dynamin-specific siRNA, we demonstrated the essential role of dynamin in the endocytosis of

MSRV entry process. Moreover, the colocalization of MSRV with dynamin detected by confocal microscopy reinforced the important role of dynamin in MSRV entry process.

Caveola-mediated endocytosis and macropinocytosis are two other endocytosis pathways that participated in the entry of viruses (3). Both clathrin- and caveolae-mediated endocytosis are dependent on dynamin, while macropinocytosis is independent of dynamin (3). Some viruses adopt more than one endocytosis pathway, such as SVCV, which enters EPC cells via clathrin-mediated endocytosis and micropinocytosis (5). Due to the requirement of dynamin in the entry of MSRV shown by our data, it indicated the potential roles of clathrin-mediated endocytosis and caveola-mediated endocytosis in the entry of MSRV into EPC cells. Further results demonstrated that the entry of MSRV in EPC cells was dependent on clathrin-mediated endocytosis rather than caveola-mediated endocytosis and micropinocytosis (Fig. 5 and 6). Additionally, some viruses may enter different types of cells through different endocytic pathways, such as Japanese encephalitis virus enters human rhabdomyosarcoma cells via clathrin-mediated endocytosis, but utilizes caveola-mediated endocytosis when infecting Jurkat T and mouse L929 cells (48). It has been reported that MSRV could infect diverse cells, including EPC, grass carp ovary cells, and largemouth bass skin cells (49), but understanding whether MSRV adopts the same endocytosis pathway in these cells needs further research.

Our final research question is the virus trafficking route. The classical trafficking route of clathrin-mediated endocytosis is the endosome/lysosome pathway, in which vesicular cargoes are transported along endocytic vesicles, early endosomes, late endosomes, or lysosomes (3). By using DiD-labeled MSRV and staining the endosomes/lysosomes with specific markers, we identified the virus trafficking route. The incoming of MSRV virions entered into early endosomes within 5 min; after that, MSRV virions were delivered into late endosomes (15 min); finally, virus particles reached lysosome (30 min). In this process, Rab5 and Rab7 GTPases are key transport regulators of early and late endosomes. Accumulating evidence also demonstrated that the entry of some members of rhabdoviruses into host cells depends on Rab5, or/and Rab7, including IHNV (22), RABV (15), and BEFV (45). Here, downregulating Rab5 and Rab7 with siRNA showed that Rab5 and Rab7 were required for the trafficking of MSRV virions following endocytosis. Moreover, the colocalization of MSRV virions with Rab5 or Rab7 supported the conclusion that Rab5 or Rab7 was involved in MSRV endocytosis. Overall, the data confirmed that MSRV traffics from early endosomes to late endosomes and further into lysosomes to initiate an infectious cycle, a process which is dependent on Rab5 and Rab7.

In the present study, using single-virus tracking, we comprehensively revealed the dynamic interaction of MSRV, clathrin, microtubule, early/late endosomes, and lysosomes. Our results provide concrete evidence that MSRV entry occurs by pH-, dynamin-, and microtubule-dependent, clathrin-mediated endocytosis pathway, and that it traffics via the endosome/lysosome pathway.(Fig. 10) Clarification of the entry pathway of MSRV will promote our understanding about the cellular entry mechanism of rhabdoviruses and provide insight into the development of novel therapeutic approaches.

MATERIALS AND METHODS

Cell culture, virus propagation, and purification

The EPC cell line used in this study was maintained in M199 medium (Gibco, Carlsbad, USA) supplemented with 10% fetal bovine serum (Gibco) and antibiotics (100 U/mL penicillin and 100 mg/mL streptomycin) at 25°C.

MSRV (MSRV-YH01, GenBank accession no. MK397811.2) was kindly provided by Jiayun Yao, Zhejiang Institute of Freshwater Fisheries, Huzhou City, Zhejiang province, China. The culture conditions for the EPC cells and the MSRV strain have been described in previous studies (25).

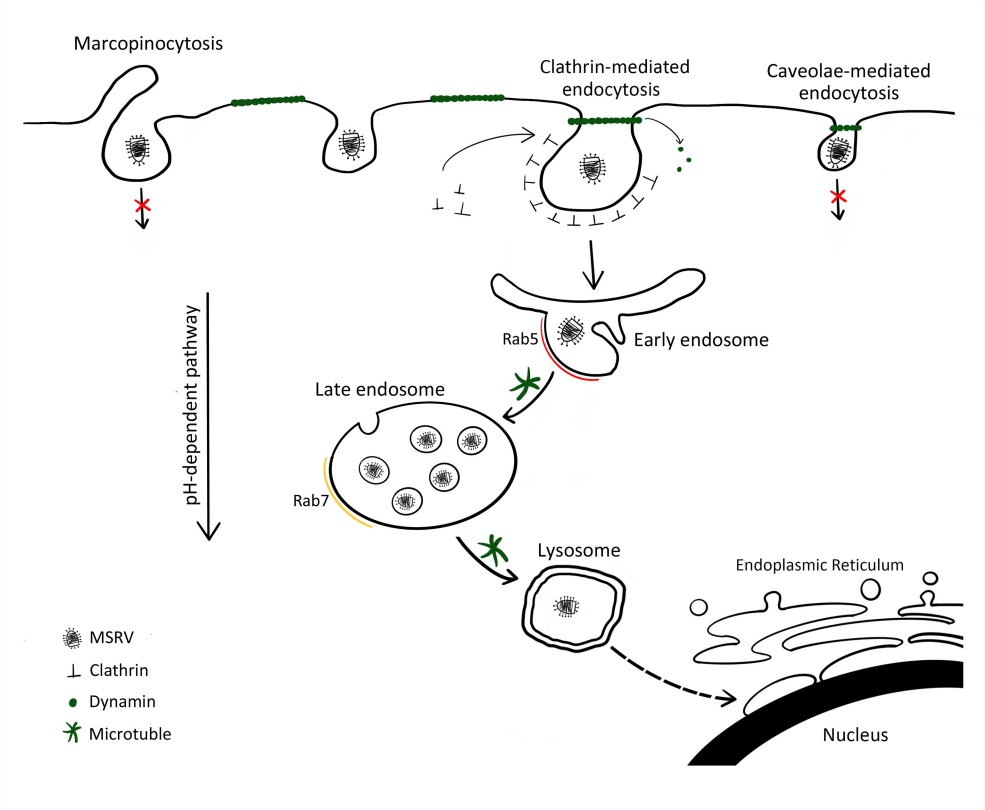

FIG 10 Models of cellular entry and trafficking of MSRV in EPC cells. MSRV attaches cell surface and is internalized from the plasma membrane via clathrin-mediated endocytosis. The virus-containing clathrin-coated vesicle is taken up into Rab5-containing early endosomes in a clathrin-, dynamin-, microtubule-, and Rab5-dependent manner. Through endosome maturation, the virus-containing endosomes acquire Rab7 and become luminal components of Rab7-containing late endosomes. Late endosomes fuse with lysosomes and transport the virus to lysosomes. The low pH of the endosomal system is required for MSRV internalization and the subsequent transport steps.

MSRV with 0.1 MOI was propagated in confluent monolayers of EPC cells. After a few days of infection, once the cytopathic effect (CPE) was sufficient, the supernatant containing MSRV was collected and viral purification was implemented. The virus was rapidly frozen and thawed three times. Viral supernatant was centrifuged at 8,000 × *g* for 20 min at 4°C to remove cell debris, and then centrifuged at 120,000 × *g* for 2 h at 4°C to concentrate viruses. After being suspended in TN buffer (50 mM Tris-HCl, 150 mM NaCl, pH 7.5), the virus was purified using a gradient of 15% to 60% (wt/vol) sucrose at 120,000 × *g* for 2 h. The resulting virus bands in sucrose solution were collected and centrifuged to remove sucrose.

Reagents

CPZ, MIBA, hyperosmotic sucrose, and NH_4Cl were purchased from Sigma-Aldrich (St. Louis, USA). Nystatin, genistin, CQ, blebbistatin, dynasore, and nocodazole were purchased from MCE (Monmouth, USA). Lyso-tracker green, lipophilic tracer DiD, tubulin-tracker, lipofectamine 3000, and Opti-MEM were purchased from Thermo Fisher Scientific (Carlsbad, USA). N protein polyclonal antibody was kept in our lab. LAMP2 polyclonal antibody was purchased from Thermo Fisher Scientific. β-actin monoclonal antibodies and HRP-conjugated goat anti-mouse IgG were supplied by ABclonal (Wuhan, China).

MSRV labeling

MSRV was labeled with DiD according to the manufacturer's instructions. Briefly, the purified MSRV particles were incubated with 10 mM DiD with gentle shaking for 2 h in dark at room temperature. Upon completion of labeling, unincorporated DiD was removed by buffer exchange into the phosphate-buffered saline (PBS) using NAP-10 filtration column (GE Healthcare, USA). The titer of the labeled MSRV particles was determined in EPC cells.

Transmission electron microscope

The morphology of DiD-MSRV virions and unlabeled MSRV virions were analyzed by TEM. The purified MSRV and DiD-MSRV were adsorbed on carbon-coated copper grids and negatively stained with 2% (wt/vol) phosphotungstic acid (PTA, pH 6.8). Then, the prepared copper grids were observed under Hitachi SU8010 TEM (Tokyo, Japan).

Virus tracking and analysis

In order to track the single-virus particle movement during virus entry into live cells, EPC cells were grown on the confocal dish, after DiD-MSRV was added to the cultured cells, the cells were placed in the CLSM cell culture room (25°C) for live cell imaging. Take video with Zeiss LSM880 microscope (Carl Zeiss, Jena, Germany). Fluorescence was excited at wavelengths of 633 nm, and images were captured at 3.726 s intervals, up to 10 min. Trajectories and velocities were measured using ImageJ software. The movement of the fluorescence was analyzed by mean-squared displacement (MSD) against time plots.

Cell viability assay

Cytotoxic effects of all inhibitors were determined by cell counting Kit 8 (CCK-8) (Beyotime, Hangzhou, China). First, EPC cells were pretreated with different concentrations of inhibitors for 24 h. After incubation, the inhibitors were removed and a 10-µL CCK-8 reagent was added for 2 h. The optical density was measured at 450 nm by microplate reader (Potenov, Beijing, China).

Internalization and replication assays

For the replication experiments, EPC cells were seeded in 24-well plates and grown overnight at 25°C. Then, cells were pretreated with the indicated concentration of inhibitors for 2 h at 25°C. MSRV was added at an MOI of 0.1 in the presence of the drugs. After 2 h of incubation, washing the cells with M199 medium, the cells were subsequently cultured with M199 containing 2% FBS at 25°C for 24 h. The cells were collected and subjected to detect viral copy by RT-qPCR or viral protein by WB.

For the internalization assays, EPC cells seeded in confocal dish were treated with different concentrations of inhibitors for 2 h at 25°C. After precooling with 4°C PBS, the cells were infected with DID-labeled MSRV at an MOI of 50 at 4°C for 30 min. The unincorporated virus by PBS was removed, and the cells were subsequently cultured with medium containing 2% FBS at 25°C for 30 min. Finally, the cells were fixed with 4% paraformaldehyde and photographed using LSM880. To monitor the effect of inhibitors, the fluorescence intensities of DID-labeled-MSRV were quantified by averaging the pixel intensities of representative cells by using ImageJ software. A total of 10 micrographs at 100× magnification were randomly selected to determine the internalization percentage of cells.

Plasmid construction and transfection

The sequences of *CLC* (accession number XM_019108370.2), *dynamin-1* (accession number XM_042751545.1), *caveolin-1* (*Cav*) (accession number XM_019082172.2), *Rab-5* (accession number XM_042776625.1), and *Rab-7* (accession number XM_019098402.2) genes were amplified by reverse transcriptase PCR from EPC cells and then inserted into

pEGFP-N1 (Clontech, Palo Alto, USA), respectively, to generate the recombinant plasmids pEGFP-CLC, pEGFP-Dyn, pEGFP-Cav, pEGFP-Rab5, and pEGFP-Rab7. The primers have been listed in Table S1.

EPC cells that grew to approximately 70–80% confluence in dishes were transfected using lipofectamine 3000 (Invitrogen, Carlsbad, USA). Briefly, 1 µg of each recombinant plasmid and 2 µL of P3000 were diluted in 50 µL of Opti-MEM and combined with 50 µL of Opti-MEM containing 2 µL lipofectamine 3000. After 15 min incubation at room temperature, the DNA-lipid complexes were added to the EPC cells, and cell cultures were incubated for 6 h at 25°C. After 6 h incubation, the medium was replaced by complete medium. After 24–48 h incubation, cells were subjected to further assays.

Western blotting

The cell extracts were collected for WB. Cell lysates were fractionated by 12% sodium dodecyl sulfate-polyacrylamide gel electrophoresis (SDS-PAGE) and transferred into 0.45 µm polyvinylidene difluoride membrane (Merck Millipore, Darmstadt, Germany). Membrane was blocked with 5% nonfat milk and incubated with indicated primary antibody. Next, the membrane was incubated with HRP conjugated secondary antibody. Finally, the membrane was conducted by ECL WB analysis kit (Thermo Fisher, USA). In order to determine protein level, optical density of the bands was quantified by ImageJ software.

Real-time quantitative PCR

Total RNA was extracted by TRIzol reagent (Invitrogen). cDNA synthesis was carried using Transcriptase M-MLV Kit (TaKaRa, Dalian, China). Quantitative PCR was performed on the ABI QuantStudio 3 Real-Time PCR System (Applied Biosystems, Foster City, USA) using TB Green Premix Ex Taq (Takara). The target genes were calculated by the $2^{-\triangle\triangle CT}$ method. Data were presented as gene expression levels normalized with β-actin or as fold changes in comparison to the control group.

Statistical analysis

All data were presented as means of the standard deviations (SD) and were performed by one-way ANOVA using IBM SPSS 22.0. Statistical significance of the difference between groups is denoted by asterisks (*, $P < 0.05$; **, $P < 0.01$).

ACKNOWLEDGMENTS

The project was supported by the Program of the National Natural Science Foundation of China (31902412), the Natural Science Foundation of Zhejiang Province (LY23C190001), and the Program of Science and Technology Department of Ningbo City (2022S156).

J.C. contributed to the conceptualization, project administration, and writing—review and editing. J.-F.L. contributed to the funding acquisition, investigation, methodology, and writing—original draft. S.L. contributed to the investigation, methodology, and data curation. H.T., J.-H.L., and Y.-F.Z. contributed to the investigation, resources, and software. Y.H. and G.-J.Y. contributed to the validation and writing—review and editing.

We declare no conflict of interest.

AUTHOR AFFILIATIONS

[1]State Key Laboratory for Managing Biotic and Chemical Threats to the Quality and Safety of Agro-products, Ningbo University, Ningbo, China
[2]Laboratory of Biochemistry and Molecular Biology, School of Marine Sciences, Ningbo University, Ningbo, China
[3]Key Laboratory of Marine Biotechnology of Zhejiang Province, Ningbo University, Ningbo, China

AUTHOR ORCIDs

Jian-Fei Lu http://orcid.org/0000-0003-0543-0109

FUNDING

Funder	Grant(s)	Author(s)
MOST | National Natural Science Foundation of China (NSFC)	31902412	Jian-Fei Lu
MOST | NSFC | NSFC-Zhejiang Joint Fund | 浙江省科学技术厅 | Natural Science Foundation of Zhejiang Province (ZJNSF)	LY23C190001	Jian-Fei Lu
program of science and technology department of ningbo city	2022S156	Jian-Fei Lu

AUTHOR CONTRIBUTIONS

Jian-Fei Lu, Funding acquisition, Investigation, Methodology, Writing – original draft | Sheng Luo, Data curation, Investigation, Methodology | Hao Tang, Investigation, Resources, Software | Jia-Hui Liang, Investigation, Resources, Software | Yi-Fan Zhao, Investigation, Resources, Software | Yang Hu, Validation, Writing – review and editing | Guan-Jun Yang, Validation, Writing – review and editing | Jiong Chen, Conceptualization, Project administration

ADDITIONAL FILES

The following material is available online.

Supplemental Material

Additional experimental details (JVI00714-23-s0001.docx). Fig S1, Table S1, and Videos S1 and S2 legends.
Video S1 (JVI00714-23-s0002.avi). The movement of DiD-MSRV in EPC cells.
Video S2 (JVI00714-23-s0003.avi). DiD-MSRV transport along microtubules.

REFERENCES

1. Marsh M, Helenius A. 2006. Virus entry: open sesame. Cell 124:729–740. https://doi.org/10.1016/j.cell.2006.02.007
2. Blissard GW, Theilmann DA. 2018. Baculovirus entry and egress from insect cells. Annu Rev Virol 5:113–139. https://doi.org/10.1146/annurev-virology-092917-043356
3. Mercer J, Schelhaas M, Helenius A. 2010. Virus entry by endocytosis. Annu Rev Biochem 79:803–833. https://doi.org/10.1146/annurev-biochem-060208-104626
4. Mercer J, Lee JE, Saphire EO, Freeman SA. 2020. SnapShot: enveloped virus entry. Cell 182:786–786. https://doi.org/10.1016/j.cell.2020.06.033
5. Shao L, Zhao J, Zhang H. 2016. Spring viraemia of carp virus enters grass carp ovary cells via clathrin-mediated endocytosis and macropinocytosis. J Gen Virol 97:2824–2836. https://doi.org/10.1099/jgv.0.000595
6. Sieczkarski SB, Whittaker GR. 2002. Dissecting virus entry via endocytosis. J Gen Virol 83:1535–1545. https://doi.org/10.1099/0022-1317-83-7-1535
7. Yamauchi Y, Helenius A. 2013. Virus entry at a glance. J Cell Sci 126:1289–1295. https://doi.org/10.1242/jcs.119685
8. Li Y, Wang J, Hou W, Shan Y, Wang S, Liu F, Moscona A. 2021. Dynamic dissection of the endocytosis of porcine epidemic diarrhea coronavirus cooperatively mediated by clathrin and caveolae as visualized by single-virus tracking. mBio 12:e00256-21. https://doi.org/10.1128/mBio.00256-21
9. Guo Y, Duan M, Wang X, Gao J, Guan Z, Zhang M. 2019. Early events in rabies virus infection-attachment, entry, and intracellular trafficking. Virus Res 263:217–225. https://doi.org/10.1016/j.virusres.2019.02.006
10. Rothman JE. 1994. Mechanisms of intracellular protein transport. Nature 372:55–63. https://doi.org/10.1038/372055a0
11. Etienne-Manneville S, Hall A. 2002. Rho GTPases in cell biology. Nature 420:629–635. https://doi.org/10.1038/nature01148
12. Brass AL, Dykxhoorn DM, Benita Y, Yan N, Engelman A, Xavier RJ, Lieberman J, Elledge SJ. 2008. Identification of host proteins required for HIV infection through a functional genomic screen. Science 319:921–926. https://doi.org/10.1126/science.1152725
13. Bucci C, Parton RG, Mather IH, Stunnenberg H, Simons K, Hoflack B, Zerial M. 1992. The small GTPase Rab5 functions as a regulatory factor in the early endocytic pathway. Cell 70:715–728. https://doi.org/10.1016/0092-8674(92)90306-w
14. Wu Q-M, Liu S-L, Chen G, Zhang W, Sun E-Z, Xiao G-F, Zhang Z-L, Pang D-W. 2018. Uncovering the Rab5-independent autophagic trafficking of influenza a virus by quantum-dot-based single-virus tracking. Small 14:e1702841. https://doi.org/10.1002/smll.201702841
15. Ahmad W, Li Y, Guo Y, Wang X, Duan M, Guan Z, Liu Z, Zhang M. 2017. Rabies virus co-localizes with early (Rab5) and late (Rab7) endosomal proteins in neuronal and SH-SY5Y cells. Virol Sin 32:207–215. https://doi.org/10.1007/s12250-017-3968-9
16. Martin-Sancho L, Tripathi S, Rodriguez-Frandsen A, Pache L, Sanchez-Aparicio M, McGregor MJ, Haas KM, Swaney DL, Nguyen TT, Mamede JI, Churas C, Pratt D, Rosenthal SB, Riva L, Nguyen C, Beltran-Raygoza N, Soonthornvacharin S, Wang G, Jimenez-Morales D, De Jesus PD, Moulton HM, Stein DA, Chang MW, Benner C, Ideker T, Albrecht RA, Hultquist JF, Krogan NJ, García-Sastre A, Chanda SK. 2021. Restriction factor compendium for influenza a virus reveals a mechanism for evasion of autophagy. Nat Microbiol 6:1319–1333. https://doi.org/10.1038/s41564-021-00964-2
17. Kuzmin IV, Novella IS, Dietzgen RG, Padhi A, Rupprecht CE. 2009. The rhabdoviruses: biodiversity, phylogenetics, and evolution. Infect Genet Evol 9:541–553. https://doi.org/10.1016/j.meegid.2009.02.005

18. Feng ZZ, Chu X, Han MZ, Yu CW, Jiang YS, Wang H, Lu LQ, Xu D. 2022. Rapid visual detection of *Micropterus salmoides* rhabdovirus using recombinase polymerase amplification combined with lateral flow dipsticks. J Fish Dis 45:461–469. https://doi.org/10.1111/jfd.13575
19. Li BY, Qin JC, Shen YF, Yang F, Wang T, Ling F, Wang GX. 2022. A therapeutic agent of ursolic acid demonstrates potential application in aquaculture. Virus Res 323:198965. https://doi.org/10.1016/j.virusres.2022.198965
20. Fu XZ, Lin Q, Liang HR, Liu LH, Huang ZB, Li NQ, Su JG. 2017. The biological features and genetic diversity of novel fish rhabdovirus isolates in China. Arch Virol 162:2829–2834. https://doi.org/10.1007/s00705-017-3416-z
21. Hu Y, Wang H, Liu L, Yao J, Chen J. 2022. Evaluation on the antiviral effect of natural product arctigenin against *Micropterus salmoides* rhabdovirus (MSRV) *in vitro* and *in vivo*. Aquaculture 560:738495. https://doi.org/10.1016/j.aquaculture.2022.738495
22. Liu HB, Liu Y, Liu SL, Pang DW, Xiao GF. 2011. Clathrin-mediated endocytosis in living host cells visualized through quantum dot labeling of infectious hematopoietic necrosis virus. J Virol 85:6252–6262. https://doi.org/10.1128/JVI.00109-11
23. Cureton DK, Burdeinick-Kerr R, Whelan SPJ. 2012. Genetic inactivation of COPI coatomer separately inhibits vesicular stomatitis virus entry and gene expression. J Virol 86:655–666. https://doi.org/10.1128/JVI.05810-11
24. Weir DL, Annand EJ, Reid PA, Broder CC. 2014. Recent observations on Australian bat lyssavirus tropism and viral entry. Viruses 6:909–926. https://doi.org/10.3390/v6020909
25. Lyu S-J, Yuan X-M, Zhang H-Q, Shi W, Hang X-Y, Liu L, Wu Y-L. 2019. Isolation and characterization of a novel strain (YH01) of *Micropterus salmoides* rhabdovirus and expression of its glycoprotein by the baculovirus expression system. J Zhejiang Univ Sci B 20:728–739. https://doi.org/10.1631/jzus.B1900027
26. Liu S-L, Wang Z-G, Xie H-Y, Liu A-A, Lamb DC, Pang D-W. 2020. Single-virus tracking: from imaging methodologies to virological applications. Chem Rev 120:1936–1979. https://doi.org/10.1021/acs.chemrev.9b00692
27. Wang S, Huang X, Huang Y, Hao X, Xu H, Cai M, Wang H, Qin Q, McFadden G. 2014. Entry of a novel marine DNA virus, Singapore grouper iridovirus, into host cells occurs via clathrin-mediated endocytosis and macropinocytosis in a pH-dependent manner. J Virol 88:13047–13063. https://doi.org/10.1128/JVI.01744-14
28. Piccinotti S, Whelan SPJ. 2016. Rabies internalizes into primary peripheral neurons via clathrin coated pits and requires fusion at the cell body. PLoS Pathog 12:e1005753. https://doi.org/10.1371/journal.ppat.1005753
29. Wang T, Wang L, Li W, Hou X, Chang W, Wen B, Han S, Chen Y, Qi X, Wang J. 2023. Fowl adenovirus serotype 4 enters leghorn male hepatocellular cells via the clathrin-mediated endocytosis pathway. Vet Res 54:24. https://doi.org/10.1186/s13567-023-01155-z
30. Macia E, Ehrlich M, Massol R, Boucrot E, Brunner C, Kirchhausen T. 2006. Dynasore, a cell-permeable inhibitor of dynamin. Dev Cell 10:839–850. https://doi.org/10.1016/j.devcel.2006.04.002
31. Li M, Zhang D, Li CT, Zheng ZF, Fu M, Ni FF, Liu YL, Du T, Wang HZ, Griffin GE, Zhang MD, Hu QX. 2020. Characterization of zika virus endocytic pathways in human glioblastoma cells. Front Microbiol 11:242. https://doi.org/10.3389/fmicb.2020.00242
32. Praena B, Bello-Morales R, López-Guerrero JA. 2020. HSV-1 endocytic entry into a human oligodendrocytic cell line is mediated by clathrin and dynamin but not caveolin. Viruses 12:734. https://doi.org/10.3390/v12070734
33. Kaksonen M, Roux A. 2018. Mechanisms of clathrin-mediated endocytosis. Nat Rev Mol Cell Biol 19:313–326. https://doi.org/10.1038/nrm.2017.132
34. Sheng XZ, Zhong Y, Zeng J, Tang XQ, Xing J, Chi H, Zhan WB. 2020. Lymphocystis disease virus (*Iridoviridae*) enters flounder (*Paralichthys olivaceus*) gill cells via a caveolae-mediated endocytosis mechanism facilitated by viral receptors. Int J Mol Sci 21:4722. https://doi.org/10.3390/ijms21134722
35. Guo C-J, Wu Y-Y, Yang L-S, Yang X-B, He J, Mi S, Jia K-T, Weng S-P, Yu X-Q, He J-G. 2012. Infectious spleen and kidney necrosis virus (a fish iridovirus) enters mandarin fish fry cells via caveola-dependent endocytosis. J Virol 86:2621–2631. https://doi.org/10.1128/JVI.06947-11
36. Filippini A, D'Alessio A. 2020. Caveolae and lipid rafts in endothelium: valuable organelles for multiple functions. Biomolecules 10:1218. https://doi.org/10.3390/biom10091218
37. Mercer J, Helenius A. 2012. Gulping rather than sipping: macropinocytosis as a way of virus entry. Curr Opin Microbiol 15:490–499. https://doi.org/10.1016/j.mib.2012.05.016
38. Kalia M, Khasa R, Sharma M, Nain M, Vrati S. 2013. Japanese encephalitis virus infects neuronal cells through a clathrin-independent endocytic mechanism. J Virol 87:148–162. https://doi.org/10.1128/JVI.01399-12
39. Zhang F, Guo H, Chen Q, Ruan Z, Fang Q. 2020. Endosomes and microtubles are required for productive infection in aquareovirus. Virol Sin 35:200–211. https://doi.org/10.1007/s12250-019-00178-1
40. Chen X-N, Liang Y-F, Weng Z-J, Quan W-P, Hu C, Peng Y-Z, Sun Y-S, Gao Q, Huang Z, Zhang G-H, Gong L. 2023. Porcine enteric alphacoronavirus entry through multiple pathways (caveolae, clathrin, and macropinocytosis) requires Rab GTPases for endosomal transport. J Virol 97:e0021023. https://doi.org/10.1128/jvi.00210-23
41. Hodgson JJ, Buchon N, Blissard GW. 2022. Identification of cellular genes involved in baculovirus GP64 trafficking to the plasma membrane. J Virol 96:e0021522. https://doi.org/10.1128/jvi.00215-22
42. Liu J, Yu C, Gui JF, Pang DW, Zhang QY. 2018. Real-time dissecting the entry and intracellular dynamics of single reovirus particle. Front Microbiol 9:2797. https://doi.org/10.3389/fmicb.2018.02797
43. Piccinotti S, Kirchhausen T, Whelan SPJ. 2013. Uptake of rabies virus into epithelial cells by clathrin-mediated endocytosis depends upon actin. J Virol 87:11637–11647. https://doi.org/10.1128/JVI.01648-13
44. Matlin KS, Reggio H, Helenius A, Simons K. 1982. Pathway of vesicular stomatitis virus entry leading to infection. J Mol Biol 156:609–631. https://doi.org/10.1016/0022-2836(82)90269-8
45. Cheng CY, Shih WL, Huang WR, Chi PI, Wu MH, Liu HJ. 2012. Bovine ephemeral fever virus uses a clathrin-mediated and dynamin 2-dependent endocytosis pathway that requires Rab5 and Rab7 as well as microtubules. J Virol 86:13653–13661. https://doi.org/10.1128/JVI.01073-12
46. Weir DL, Laing ED, Smith IL, Wang L-F, Broder CC. 2014. Host cell virus entry mediated by Australian bat lyssavirus G envelope glycoprotein occurs through a clathrin-mediated endocytic pathway that requires actin and Rab5. Virol J 11:40. https://doi.org/10.1186/1743-422X-11-40
47. Ferguson SM, De Camilli P. 2012. Dynamin, a membrane-remodelling GTPase. Nat Rev Mol Cell Biol 13:75–88. https://doi.org/10.1038/nrm3266
48. Liu C-C, Zhang Y-N, Li Z-Y, Hou J-X, Zhou J, Kan L, Zhou B, Chen P-Y. 2017. Rab5 and Rab11 are required for clathrin-dependent endocytosis of Japanese encephalitis virus in BHK-21 cells. J Virol 91:e01113-17. https://doi.org/10.1128/JVI.01113-17
49. Gao E-B, Chen G. 2018. *Micropterus salmoides* rhabdovirus (MSRV) infection induced apoptosis and activated interferon signaling pathway in largemouth bass skin cells. Fish Shellfish Immunol 76:161–166. https://doi.org/10.1016/j.fsi.2018.03.008